

FACILITY FORM 802

**N65-27958**

(ACCESSION NUMBER) \_\_\_\_\_ (THRU) \_\_\_\_\_

15

(PAGES) \_\_\_\_\_ (CODE) \_\_\_\_\_

CR 63774

(NASA CR OR TMX OR AD NUMBER) \_\_\_\_\_ (CATEGORY) 14

*Rochester*

**Interim Progress Report**

**Contract NASr - 14**

**December 1, 1964 to February 28, 1965**

**UNPUBLISHED PRELIMINARY DATA**

GPO PRICE \$ \_\_\_\_\_

OTS PRICE(S) \$ \_\_\_\_\_

Hard copy (HC) 1.00

Microfiche (MF) .50

## Optical Design

Richard Mostrom and Neil Hochgraf

Work on the optical design (theoretical) and evaluation (experimental) of the preliminary instrument during the last six months has been directed mainly toward the improvement of the design already described and the analysis of alternative designs. At the same time work progressed on the construction and assembly of the vacuum and optical systems to be used for grating calibration and evaluation measurements.

### Analysis of the Wide Grating

After the report for June - August, 1964 inaccuracies were discovered in the Special Purpose Ray Trace (SPRYT) and Spot Diagram Program (SAM). The errors were corrected and the programs converted for use with a cylindrical focal surface (same radius, 100.26 m/m).

Finally, eight traces were made: four for the preceding spherical focal surface (same radius) to compare with the four for the cylindrical surface, at directions of source radiation: (a) in the principle plane of the grating, inclined horizontally at  $8^{\circ}17'$  to the grating normal, (b) inclined at  $2^{\circ}$  to (a) vertically, (c) inclined to (a) at  $2^{\circ}$  horizontally away from the normal, and (d) combined conditions of (b) and (c). These spot diagrams are shown in Figures I and II. Figure I (cylindrical) and Figure II (spherical). It is evident that for the case of the largest blur (scale .24 mm/in.) case (d) at  $300 \text{ \AA}$ , the cylindrical surface better approximates the actual curved focal surface than does the spherical surface. That is,

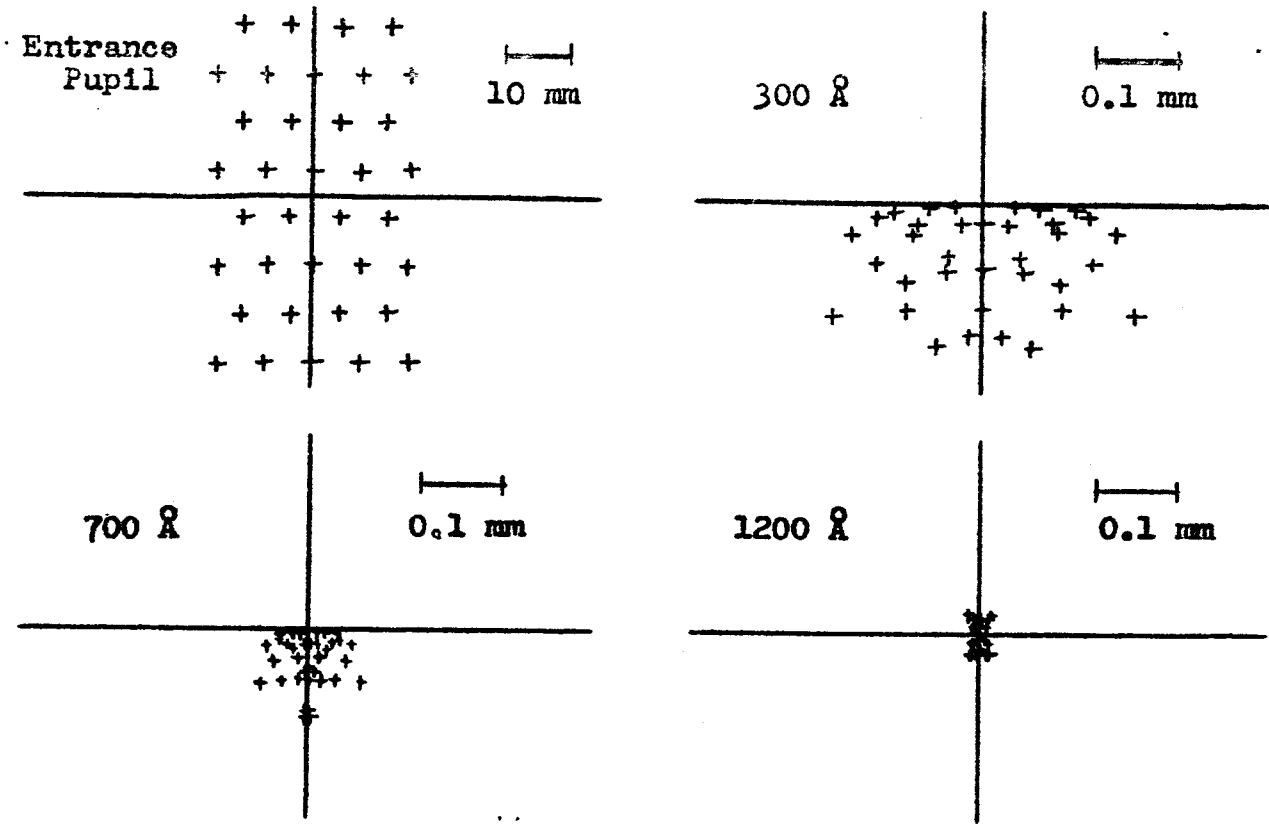


Figure 1a Spot diagrams for light incident at  $8^{\circ}17'$  horizontally to grating normal (cylindrical focal surface)

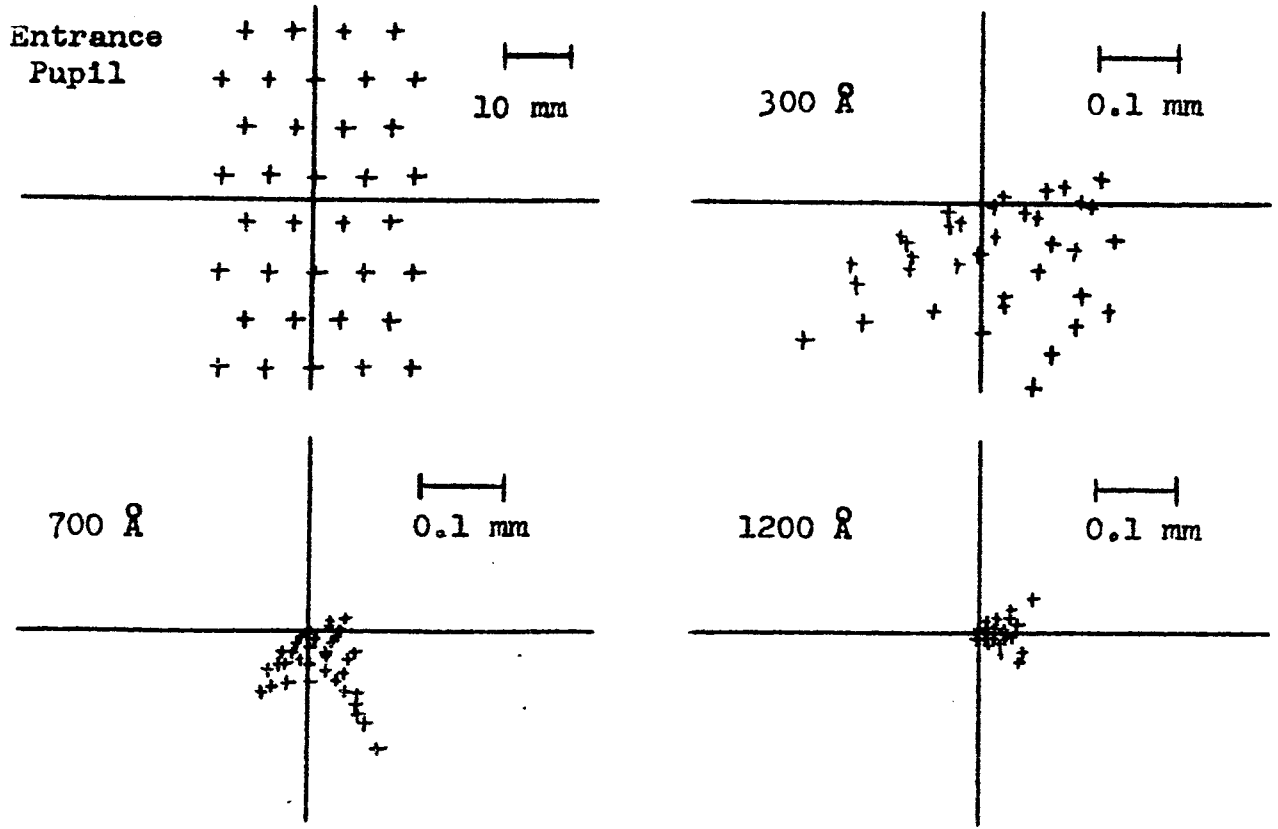


Figure 1b Spot diagrams for light incident at  $2^{\circ}$  vertically to condition in Fig. 1a (cylindrical focal surface)

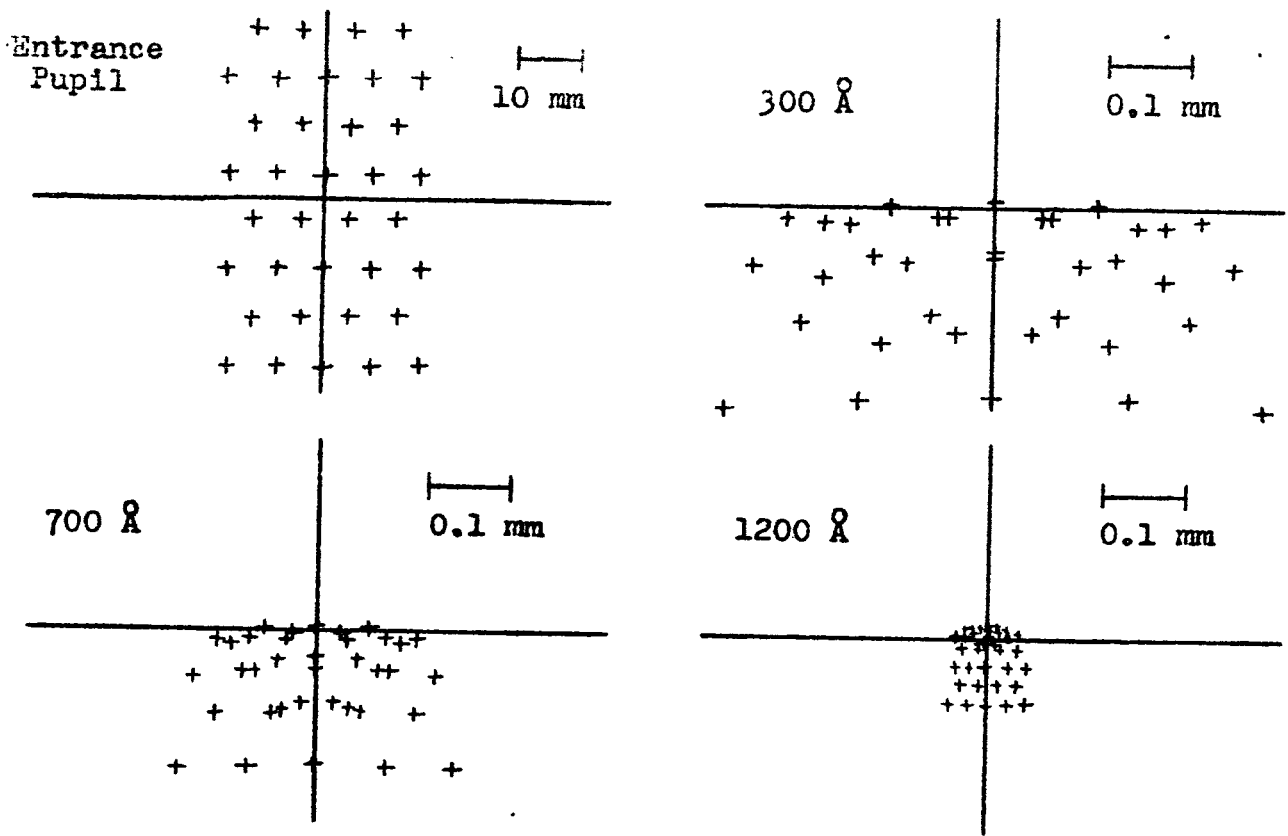


Figure 1c Spot diagrams for light incident at  $10^{\circ}17'$  horizontally to grating normal (cylindrical focal surface)

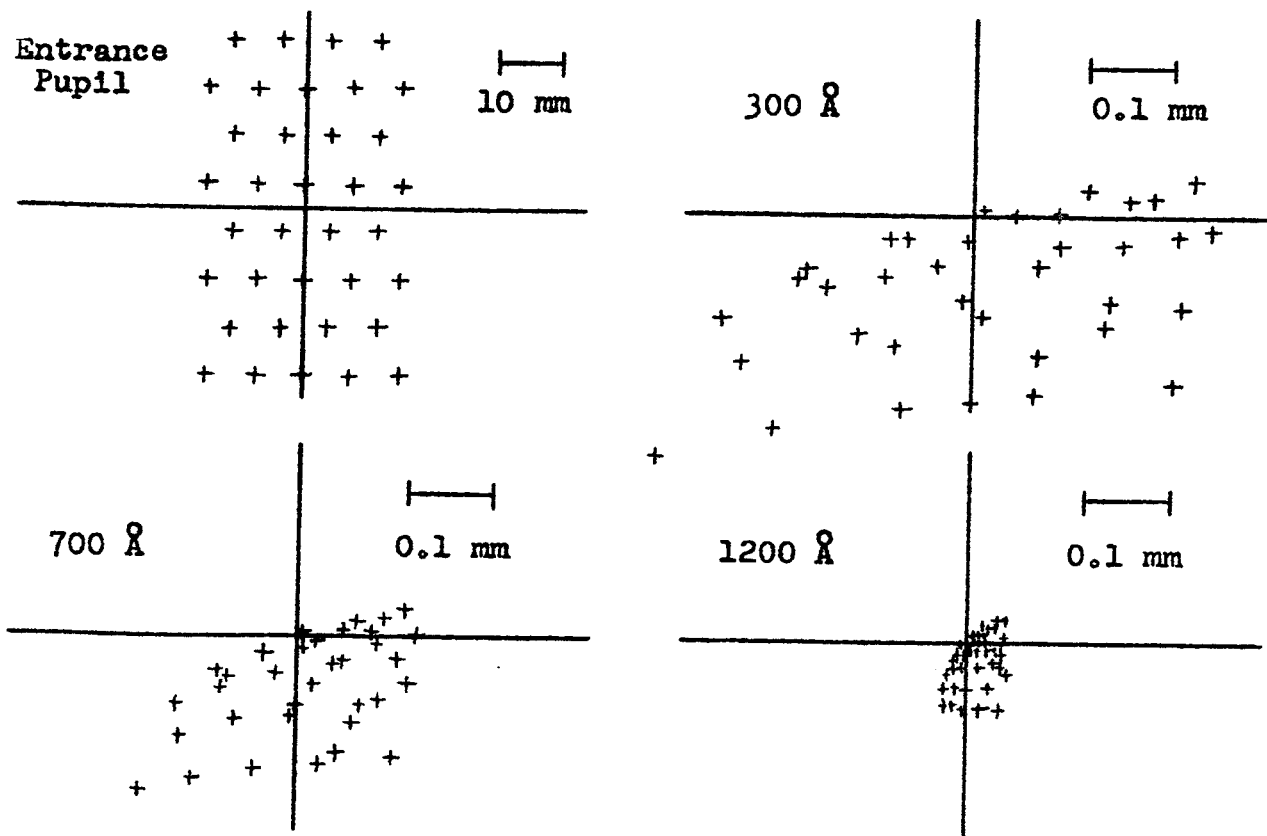


Figure 1d Spot diagrams for light incident at  $2^{\circ}$  vertically to condition in Fig. 1c (cylindrical focal surface)

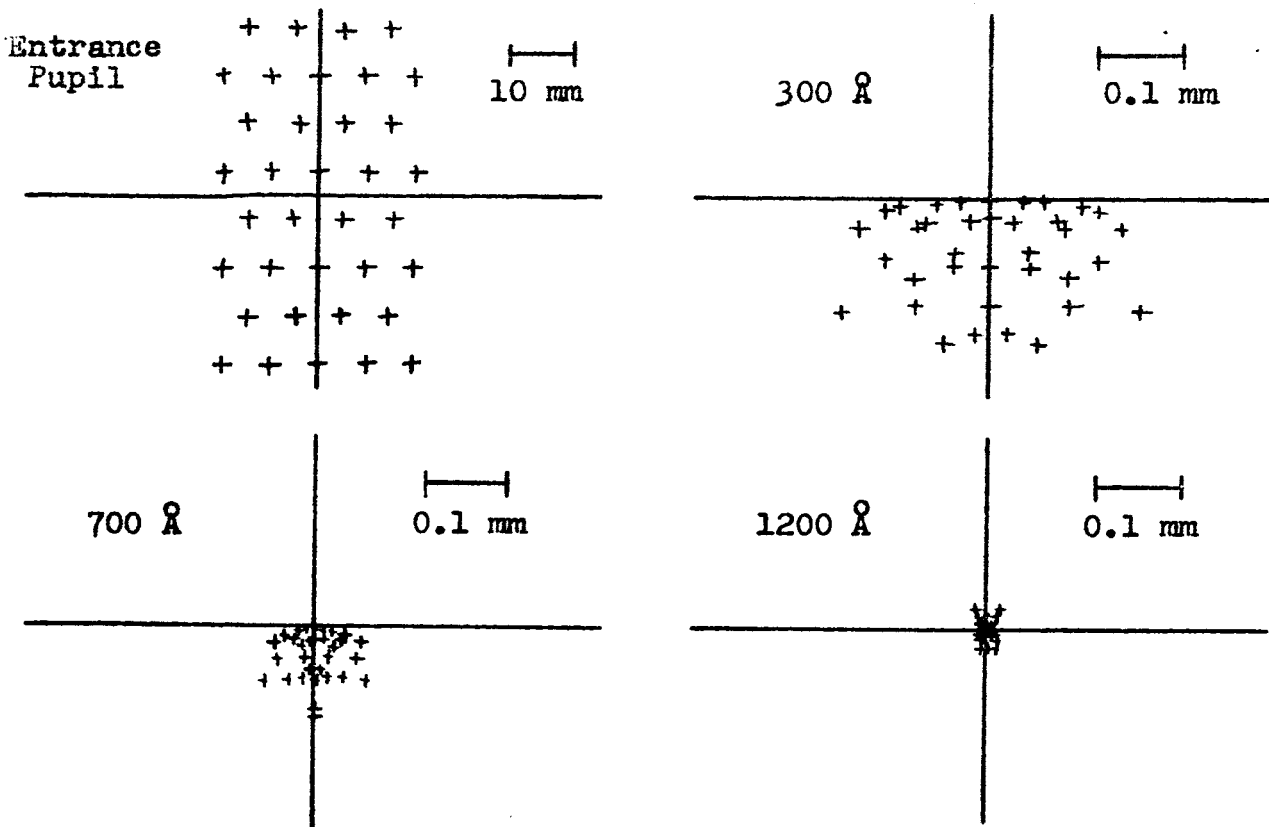


Figure IIa Spot diagrams for light incident at  $8^{\circ}17'$  horizontally to grating normal (spherical focal surface)

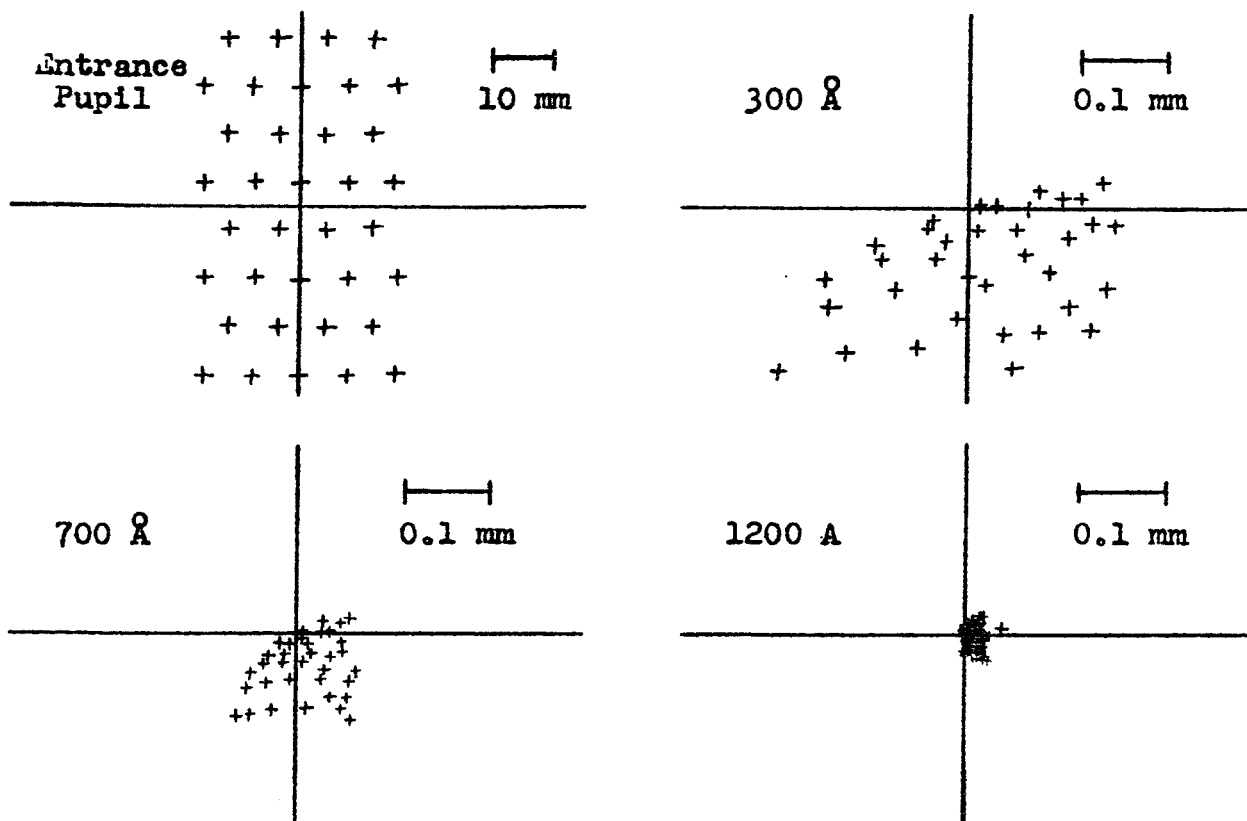


Figure IIb Spot diagrams for light incident at  $2^{\circ}$  vertically to condition in Fig. IIa (spherical focal surface)

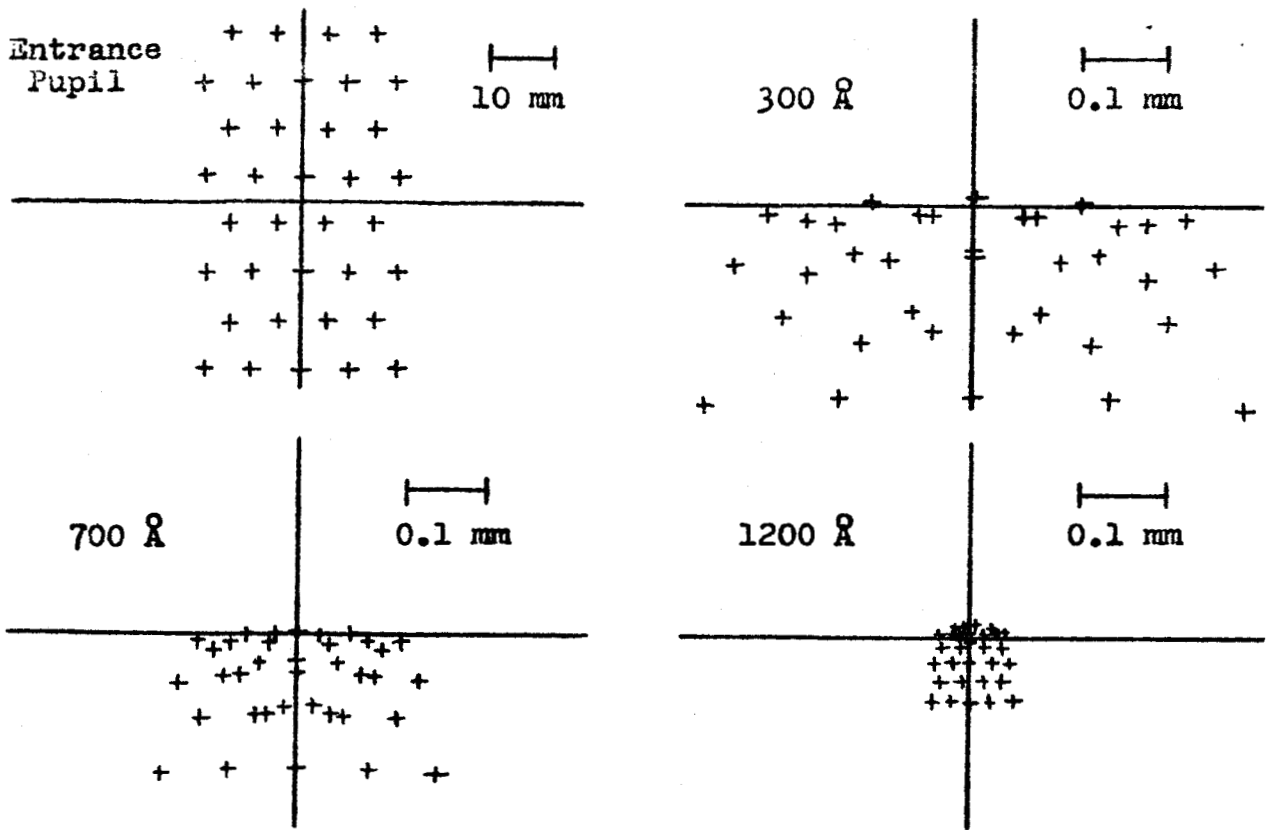


Figure IIc Spot diagrams for light incident at  $10^{\circ}17'$  horizontally to grating normal (spherical focal surface)

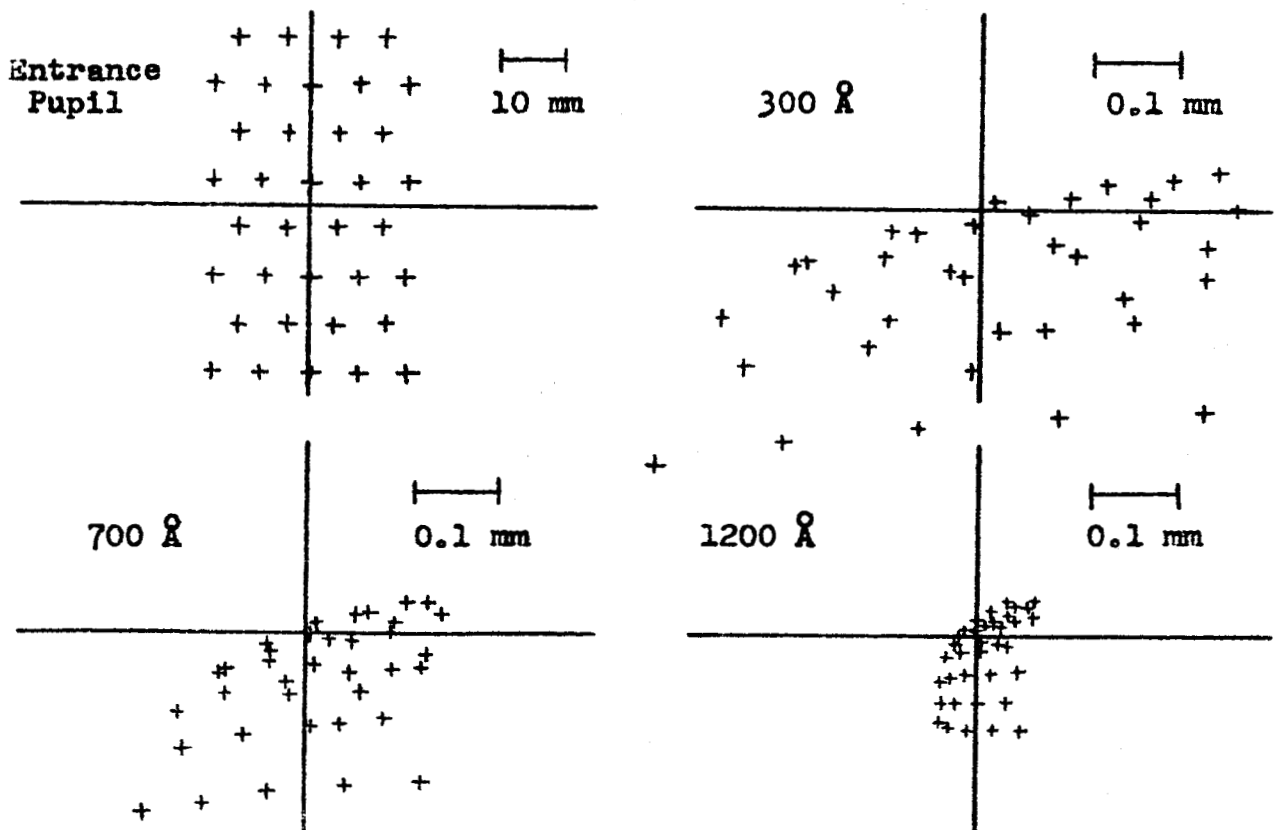


Figure IIId Spot diagrams for light incident at  $2^{\circ}$  vertically to condition in Fig. IIc (spherical focal surface)

the vertical blur which is necessary to reduce for greater exposure is less for each case of the  $300 \text{ \AA}$  line. This is the desired result, eliminating the necessity of having to bend the film into a torus or an asphere.

### Analysis of a Tall Narrow Grating

In order to reduce the baffle dimension in the direction of dispersion so that the entire baffle could be enclosed within the rocket, it was suggested that the shape of the grating be reversed by reducing the width and increasing the height to maintain the same area. This not only simplifies the baffle, it also gives a better resolved spectrum. The ray trace (case (d)) for a cylindrical surface shows that the resolution (i.e. reduction of the blur dimension in the direction of dispersion) is increased (blurr  $\sim .3 \text{ mm}$  at  $300 \text{ \AA}$ , compared to previous  $.345 \text{ mm}$ ). (See Figure III). However, light is spread into the vertical direction by the increase of the tangential astigmatism resulting from the increase of grating height. Although the vertical spread of the image is increased, the overall area of the image is still about 10% smaller, thereby improving exposure. This improvement is confirmed theoretically in H. G. Beutler, May 1945 J.O.S.A., page 344, in the search for the Wadworth's mount "optimal width". It was also noted by B & L Inc. in grating 35-52-11-72 which is actually ruled  $W=30 \text{ mm}$  x  $H=50 \text{ mm}$  or taller than wide.

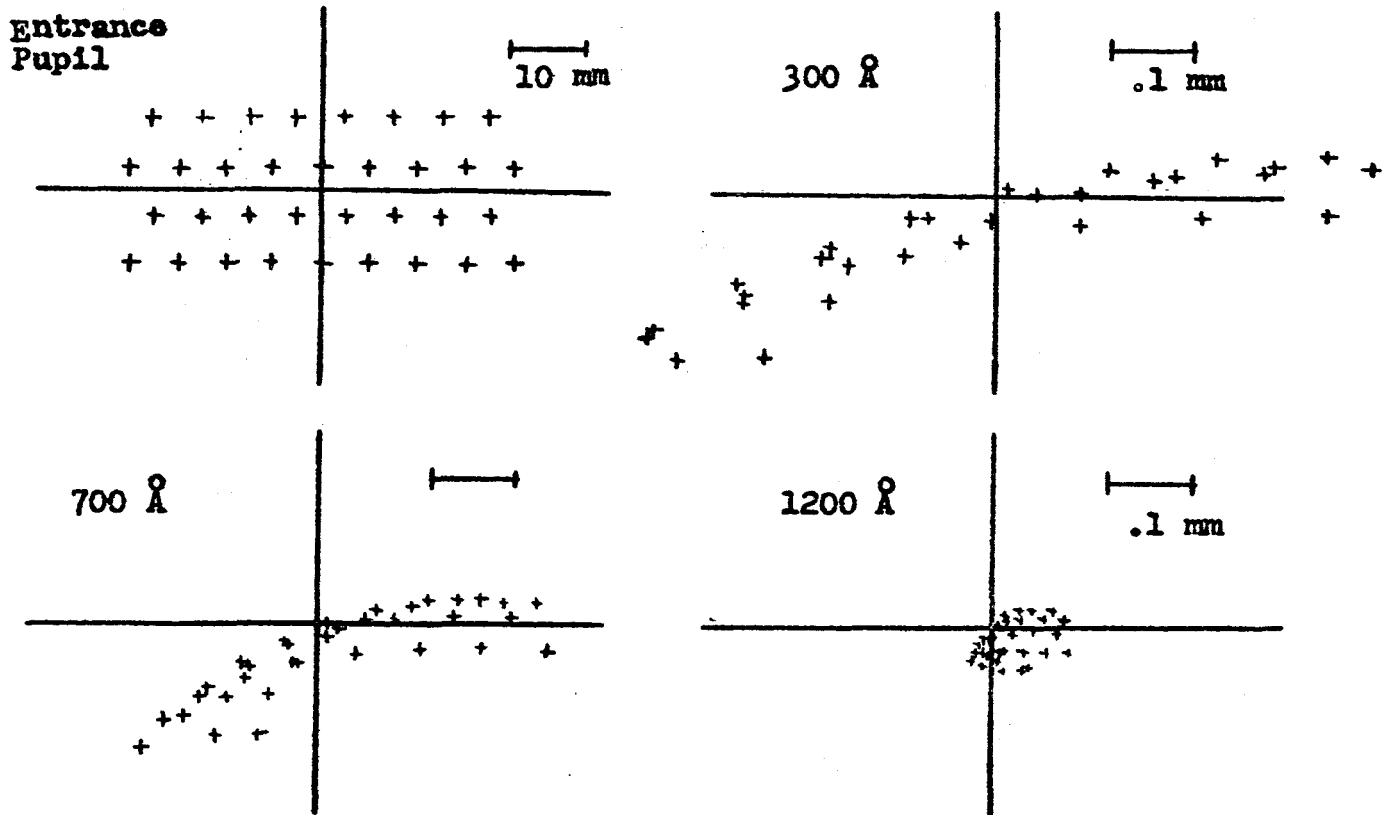


Figure III Spot diagrams for light incident at  $10^{\circ}17'$  horizontally and  $2^{\circ}$  vertically to normal grating (cylindrical focal surface with grating dimensions reversed)

#### Distorting the Grating Blank by "Pinching"

Upon careful tracing of more rays for each of the four conditions with the cylindrical surface, it may be determined whether a grating with a toroidal surface would be worth-while. This might be done by pinching the grating along the vertical sides.

Bending the grating to improve the image is neither a difficult nor dangerous thing to do since the forces and stresses ( $S_s = 500\text{psi}$ ) required are small and well within the elastic range of glass. Such a procedure was described in a local Optical Society meeting some 3 years ago. The holder described was said to maintain its corrected shape when tested interferometrically a year later. From center of grating to maximum height an angular twist of 1 min. of arc



and about 1.5 min. of arc increase in power along the vertical direction from center to edge would be required. Such bending while open to calculation would be accomplished by adjusting spring loaded screws in the grating's immediate holder, (at worst the grating could loosen and return to its unloaded shape). The adjustment is expected to be simple because the rectangular shape aperture of the grating gives 1 to 9 ratio between the focal range of the vertical to horizontal direction. This minimizes the cross talk between the respective image directions. A holder to accomplish the bending has been drawn up.

The bent grating solutions show also another desirable feature in that the image, but not the resolution, at the  $1200\text{\AA}$  end is degraded while both the image density, shape and resolution are distinctly improved progressively toward the  $300\text{\AA}$  end. This tilting of the energy vs wavelength curve should tend to put all recorded lines within the short latitude range of the film that must be used. Sufficient image density might be available now to allow a lower efficiency coating to be used<sup>1</sup> which discriminates against  $1200\text{\AA}$  -  $900\text{\AA}$  light, to reduce both this signal range as dispersed and reduce the air glow emission scatter.

The above discussion of a pinched grating points out some of the possibilities that lie in this grating, but sufficient mechanical strength has been built into the grating mount to add this feature.

#### Further Discussion of the Tall Grating

With renewed interest in the idea of a grating with a longer vertical dimension, it was determined that the maximum vertical dimension which could be utilized on the grating blank (diameter =  $3\frac{1}{4}$ " ) maintaining the same ruled area (1500 sq. m/m) would be 75 m/m. See Figure IV.

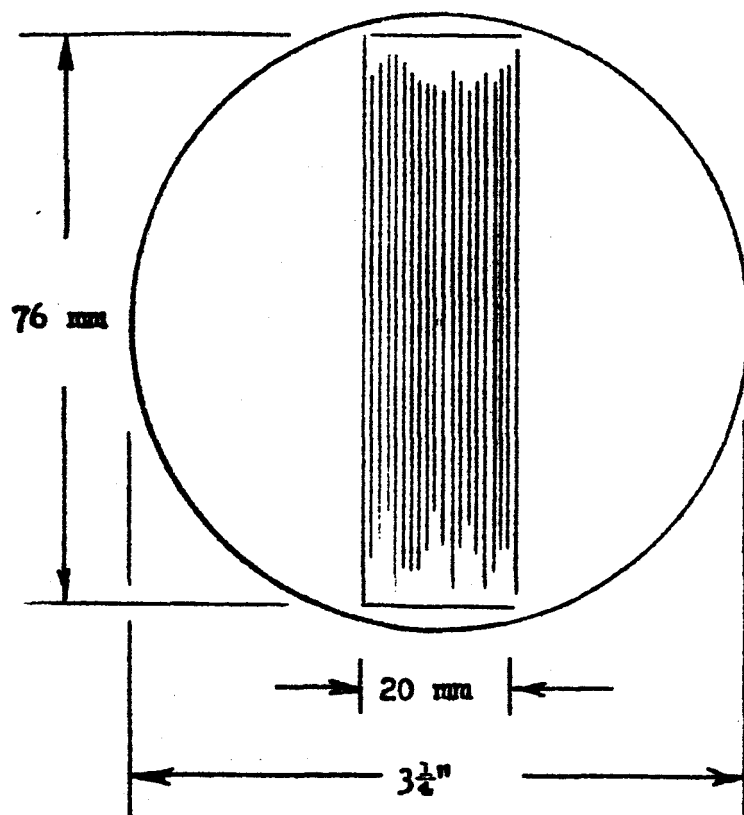


**Figure IV Actual scale of 20 x 75 mm vertically ruled grating**

Thus for a grating whose rulings measure 20 x 75 m/m, a new ray trace was made (see Figure V). This included incident light in the principle plane at the standard angle of incidence ( $8^{\circ}17'$  [case(a)]). It can be seen from the spot diagram that the tangential astigmatism in the  $300\text{\AA}$  image has increased with the increase in grating height, but that perhaps this may be reduced by refocusing.

Several refocusing traces were made by both increasing and decreasing the radius of curvature of the film surface while maintaining the axial distance from the grating. That is, only the focus of the  $300\text{\AA}$  and  $700\text{\AA}$  lines were changed. At approximately a radius of 140 m/m a very interesting feature in the image construction may be seen. (See Figure VI). That is, in the image of the  $300\text{\AA}$  line and

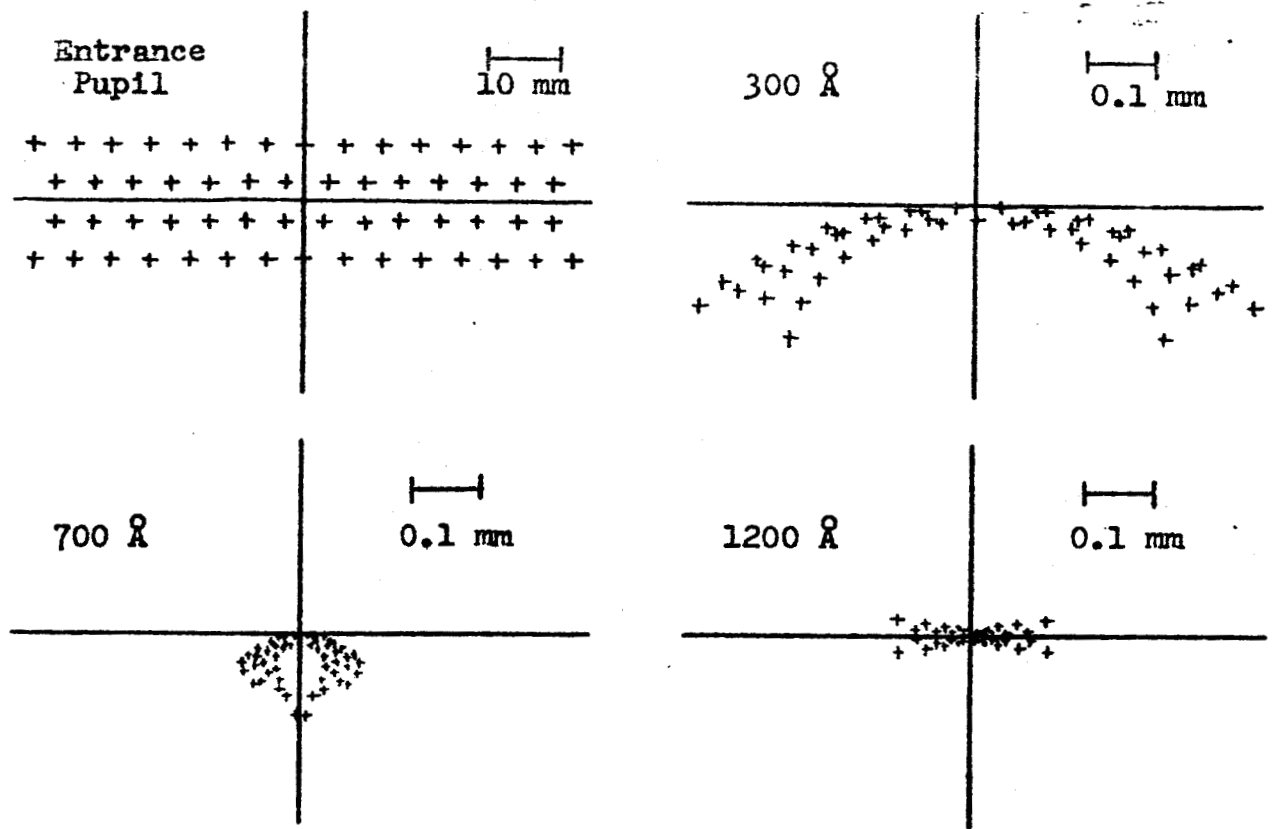


Figure V Spot diagrams for light incident at  $8^{\circ}17'$  horizontally to grating normal (cylindrical focal surface radius = 100.26 mm)

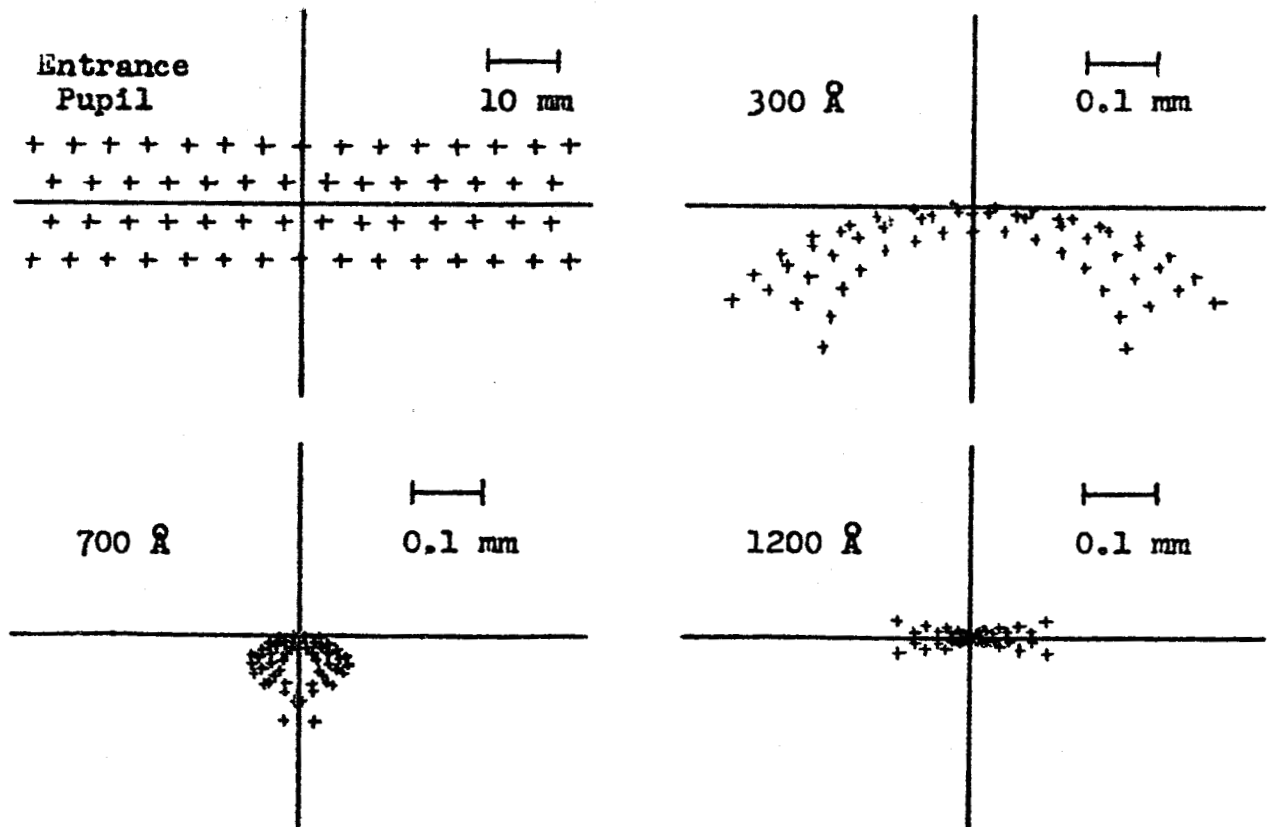


Figure VI Spot diagrams for light incident at  $8^{\circ}17'$  horizontally to grating normal (cylindrical focal surface radius = 140 mm)

and to a lesser extent in that of  $700\text{\AA}$ , the two fans of rays located farthest off axis in the positive  $x$  direction (program convention) formed a better image in the resolution direction than those to the left of the chief ray. This feature demonstrated the possible advantage in decentering the grating in the positive  $x$  direction a distance of from 1 to 2 ray fans.]

### A Tall Decentered Grating

The following spot diagrams (Figures VII and VIII) of decentered gratings ( $300\text{\AA}$  line) make quite evident the fact that the optimum amount of decentering occurs when the edge of the grating lies exactly at the center of the grating blank. This is seen from the fact that the farthest ray fan in the positive  $x$  direction (in Figure VII) corresponds to that fan in the image surface which contains the most curvature, and as a result, is farthest removed from all concentrated energy distribution. On the other hand, in Figure VIII, the same is true for the fan on the negative side of the chief ray. This fan not only detracts from the resolution, but as in the previous case, from the energy distribution. In practice it is not possible to show this condition with the ORDEALS program, since the spot diagram is plotted with only an even number of ray fans. It is an accurate estimation that the actual resolution of the stated configuration lies between 1 and  $3\text{\AA}$ .

The remaining improvement of the optical image at the low end of the spectrum of interest lies in the domain of "energy distribution improvement". It may be seen from Figure VII and VIII that the energy distribution resulting in a dense exposure for the 700 and  $1200\text{\AA}$  lines is far superior to that of the  $300\text{\AA}$  line. From an actual

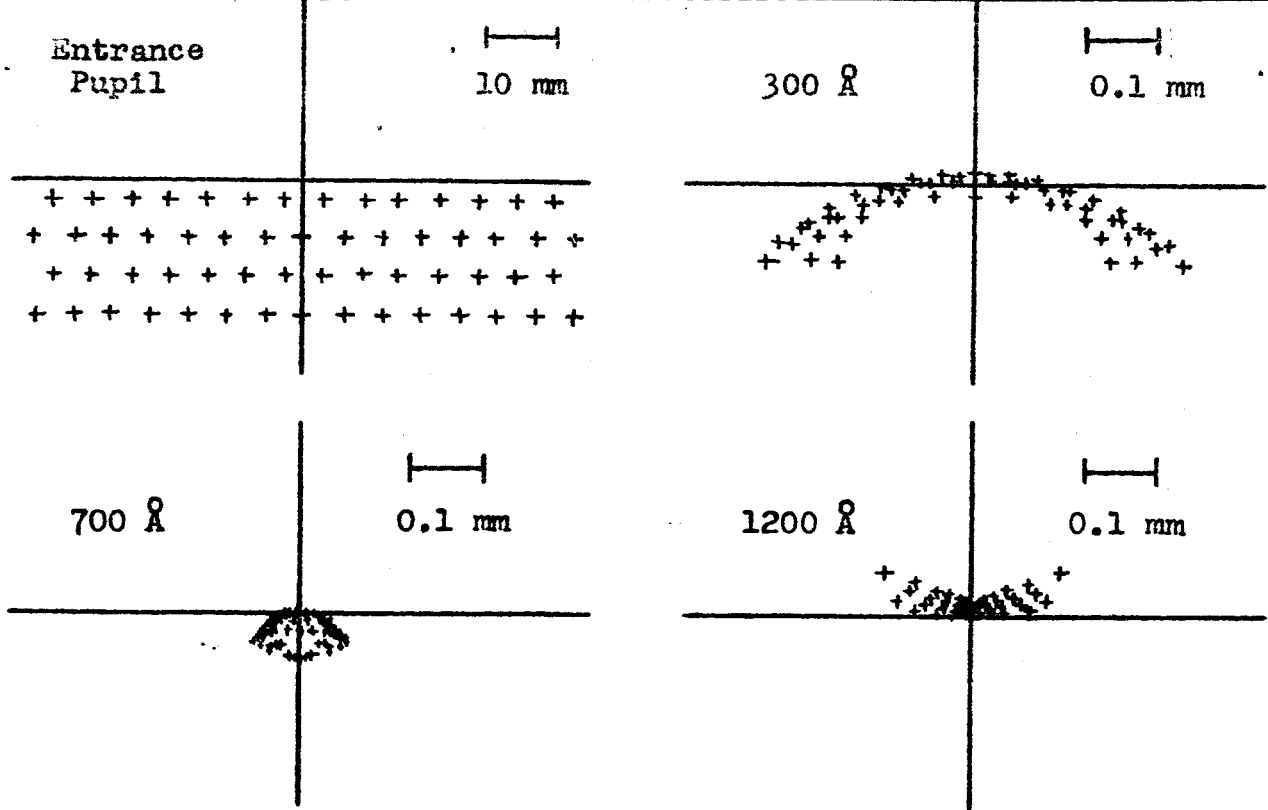


Figure VII Spot diagrams for light incident at  $8^{\circ}17'$  horizontally to grating normal (cylindrical focal surface radius = 140 mm)

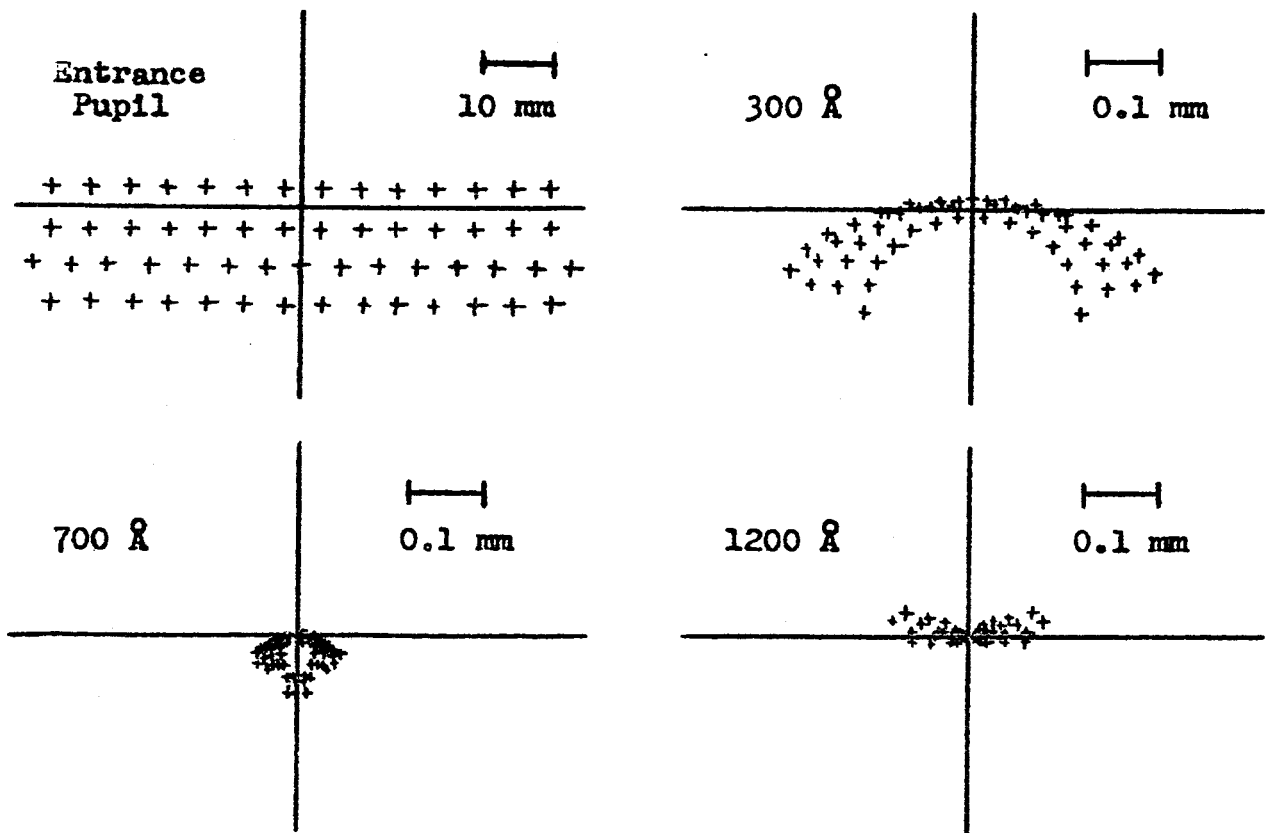


Figure VIII Spot diagrams for light incident at  $8^{\circ}17'$  horizontally to grating normal (cylindrical focal surface radius = 140 mm)

listing of each ray in the image surface (provided by output spot list), corresponding to that in the object surface, it was determined that rays received from the center edge portion of the entrance pupil detracted from the resolution, but those from the outer edge didn't detract badly from the energy distribution.

As a result, a ray trace was made with an entrance pupil of increased width from which the undesirable rays were deleted (as in Figure IX). Thus, if we mask the aperture as shown in Figure IX, we not only will improve the energy distribution of the image of the  $300\text{\AA}$  line, but in maintaining the same area of the entrance pupil, the resolution of each of the three lines will be improved as well.

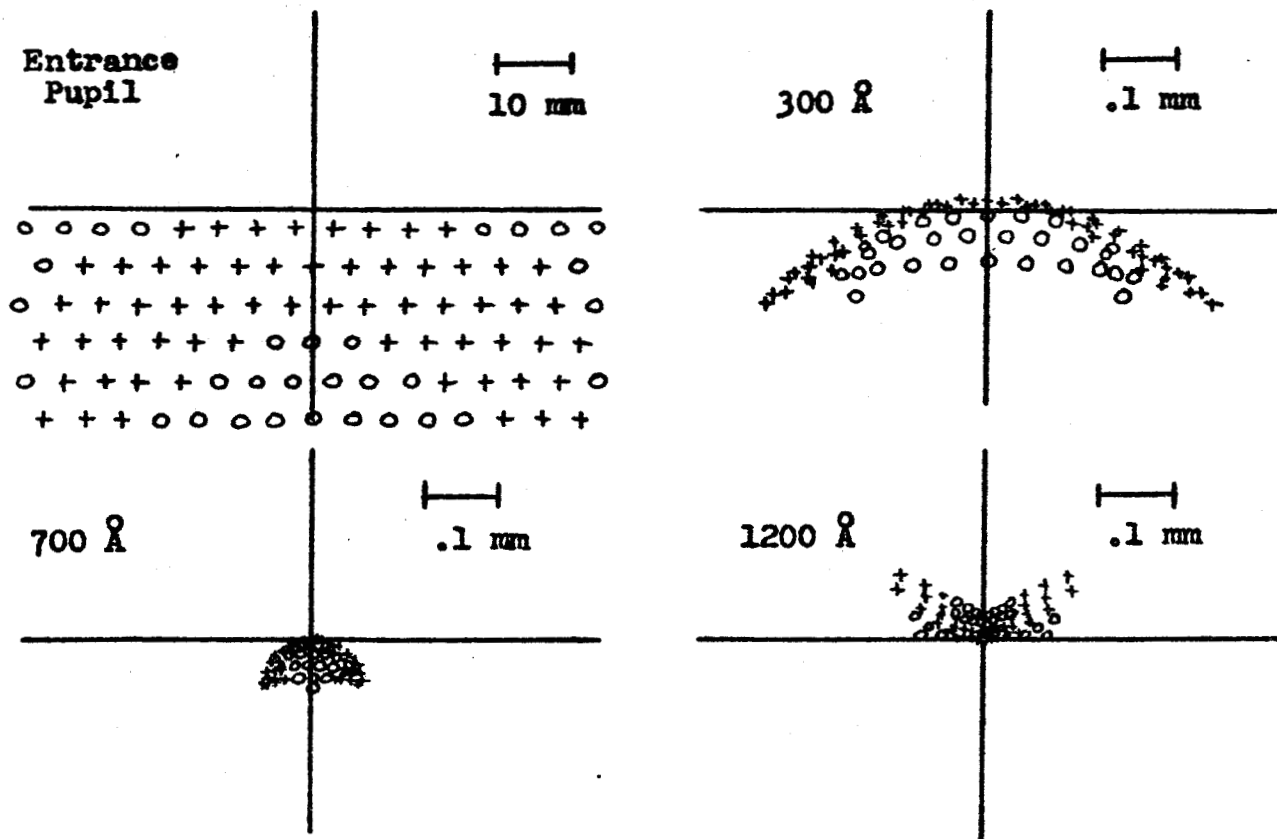


Figure IX Spot diagrams for crescent shape grating light incident at  $8^{\circ}17'$  horizontally to grating normal (deleted rays designated by 0)

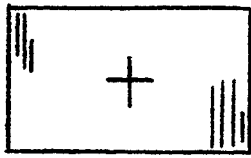
In conclusion, the comparison of Figure Ia, Figure V and Figure IX in Figure X shows the progressive improvement of the resolution from the original 30 x 50mm aperture through the reversed 75 x 20mm to the defocused, decentered crescentshaped aperture of the same 1500 sq. mm area. This comparison shows that the method of aperture manipulation has important ramification on the resolution and ray-image density. The original optical solution gives a safe resolution of about  $50\text{\AA}$  while improved solutions give a resolution between  $5\text{\AA}$  and  $2\text{\AA}$  with the image density being greatly improved. Hence for the same exposure on a film the exposure time could be reduced by a factor of 2 for the unbent but apodized grating in a Wadsworth solution. These improvements in exposure time are extremely valuable in that: they (1) reduce the image blur by jitter of the pointing control in proportion to the reduction in image area (assuming random jitter direction), (2) increase the number of exposures that can be taken to give a prescribed film density, (3) accomplish the above improvement to such an extent that a comparable increase in exposure rate could not be accomplished by increasing grating aperture or shortening the focal length. Advantage (2) is particularly valuable in that a wider range of exposures can compensate for the small latitude of the film. In general the most improved optical solution would allow emission and absorption lines to be recorded and in the very best circumstances their crude line profile to be obtained.

All solutions depend only on the grating-baffle actually used and these could be interchanged at any time in the rocket instrument package as designed.

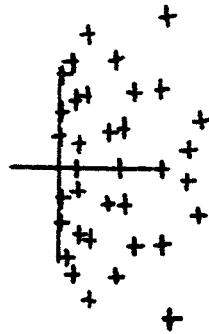
#### Reference

- 1 E.M. Reeves & W. H. Parkinson, JOSA, Vol. 53, No. 8, 941-945  
"Efficiencies of Gold & Platinum Gratings in the Vacuum Ultraviolet"

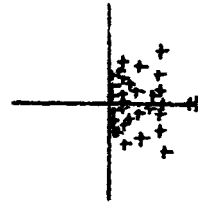
Entrance  
Pupil



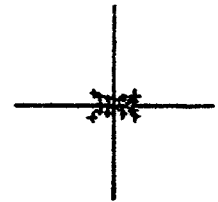
300 Å



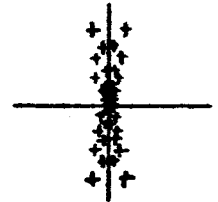
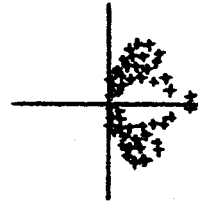
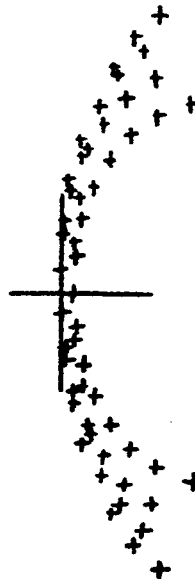
700 Å



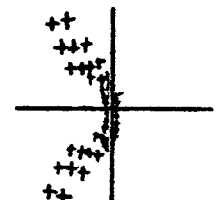
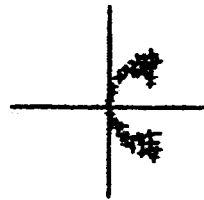
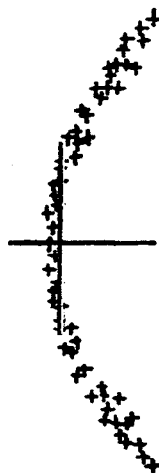
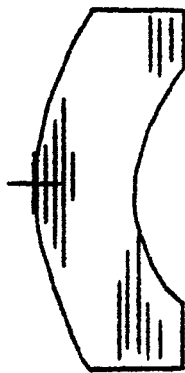
1200 Å



Max. resolution  $\sim 30$  Å image areas normalized to unity (from Fig. Ia)



Max. resolution  $\sim 4$  Å, image areas (respectively) 0.9, 2.5, 3.0  
(from Figure V)



Max. resolution  $\sim 3$  Å, image areas (respectively) 0.4, 0.5, 4.0  
(from Figure IX)

Figure X A comparison of improved image spot diagrams